



Research article

Study on high-temperature performance evaluation of asphalt mixtures with anti-rutting additives

Gang Tian^{1,2}, Ying Gao², Conglin Chen^{2,*} and Qin Ye^{1,3}

¹ National Engineering Research Center of Advanced Road Materials, Nanjing 211112, China

² School of Transportation, Southeast University, Nanjing 211189, China

³ JSTI Group Co., Ltd., Nanjing 210019, China

* **Correspondence:** Email: conglinchen@seu.edu.cn.

Abstract: In order to investigate the asphalt mixture enhancement due to the granular anti-rutting additives, the multiple stress creep recovery (MSCR) test and wheel tracking test were performed to examine the effects of three anti-rutting additives on the high-temperature performance of binders and mixtures, respectively. Further, the interaction mechanism between anti-rutting additives and asphalt binder was revealed via a fluorescence microscopy (FM) test. The results indicate that the incorporation of anti-rutting additives causes a substantial increase in elasticity behavior for binders, along with a massive enhancement of dynamic stability for mixtures. Further, the enhancement of performance is not conclusively determined by the compatibility between the additive and asphalt. Instead, unmelted viscous-flow additives contribute to the enhancement of mixtures by interlocking, filling voids, cementing and wrapping the aggregate, which are essential mechanisms of mixture modification. This study contributes to selecting appropriate additives in engineering and enhancing anti-rutting additives based on their modification mechanism.

Keywords: modified asphalt mixture; granular anti-rutting additive; mechanism of interaction; high-temperature performance; FM test; MSCR test; wheel tracking test

1. Introduction

Pavement rutting, as one of the most typical distresses in asphalt pavement, may influence driving comfort and safety [1] and even accelerate the decline of pavement serviceability [2]. The generation

of pavement rutting is primarily due to the effects of densification and shearing slip of mixtures [3], which has a strong relationship with the asphalt properties and mechanical interaction of aggregates. In order to objectively treat the rutting distress, many studies developed applicable technologies or new materials to improve the performances of asphalt binder and asphalt mixtures, including employing effective additives and optimizing gradation design and combination design [4–6]. The anti-rutting additive was considered as an efficient material to increase the rutting resistance of asphalt pavement, which could be utilized by directly mixing with mineral aggregates [7]. The asphalt mixture is viscoelastic, which implies that a high temperature will affect its stiffness and resistance to deformation. With the application of additives, the elastic or viscous behaviors will hugely change, accordingly resulting in modification on the binder and improvement of the material's structure. However, the dispersed form of anti-rutting additives in a binder and aggregate skeleton remains unclear. Therefore, the issue of high-temperature performance is an essential focus for extensive research on asphalt mixtures with anti-rutting additives.

There are many types of anti-rutting additives, typically including PR PLAST.S produced by PR. INDUSTRIE in France, composite modifiers Duroflex and Domix developed by a company in Berlin, Germany as well as SEAM developed by Shell in the United States [8]. However, these additives are different in their application conditions and effects. Zhang et al. [9] compared the improvement effects of asphalt mixtures modified with anti-rutting additives PR, RA and Duroflex, and found that the types of anti-rutting additives have a greater impact on the high-temperature performance of asphalt mixtures compared to their dosage. Further, a novel anti-rutting asphalt mixture was developed by using matrix asphalt with a penetration of 40/60, anti-rutting additive and hard basalt aggregate, which demonstrates promising practicality of road intersection maintenance [10]. Wang et al. [11] prepared a permeative anti-rutting agent based on epoxy resin and Buton rock asphalt. Han et al. [12] investigated the effects of granulated polymer anti-rutting additives on the comprehensive performance of asphalt mixtures. Xiao et al. [13] compared three binders modified with polymer additives and found that the modified asphalt with high polymer contents showed a similar performance to that of styrene–butadiene–styrene (SBS) modified asphalt.

Based on the background above, a considerable number of performance-centered researches have been conducted to investigate the mixtures' enhancement due to anti-rutting additives. However, the interaction between the mixtures and anti-rutting additives remains unclear. Besides, the studies on the effect of anti-rutting additives on the sole binder or aggregate system have not been reported yet, as they are both contributory subcomponents of the mixture. To fill this gap, this study examined the high-temperature performance of anti-rutting additives modified asphalt and asphalt mixtures. Afterward, the modification mechanism of the additive was investigated.

2. Materials and methods

To test the road performances of binders, three modified asphalts were prepared by mixing with three anti-rutting additives, respectively. Thereafter, the fluorescence microscopy (FM) test and multiple stress creep recovery (MSCR) test were performed to examine the binders' performance and compatibility. Further error analyses of the wheel tracking test were carried out to ensure the reliability of the test. Most significantly, the interaction mechanism between additives and asphalt was figured out by associating the material's performance and compatibility. The technical framework of this study is shown in Figure 1.

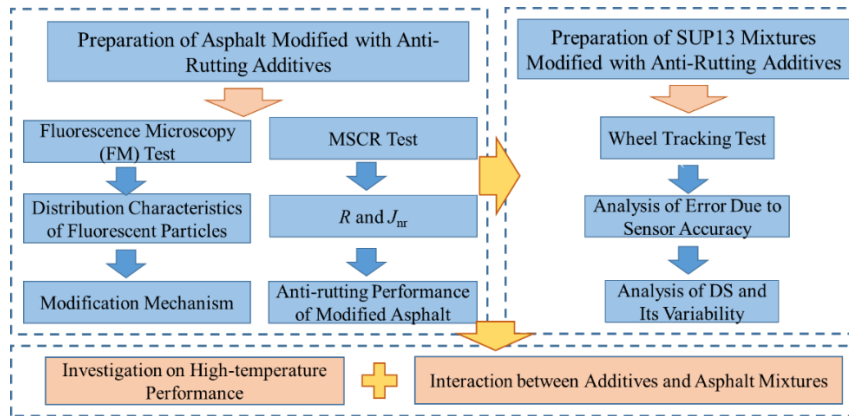


Figure 1. Technical framework of this study.

2.1. Raw materials

70# base asphalt was used to prepare modified asphalt and asphalt mixtures, and its fundamental properties were tested in the laboratory in accordance with JTG E20-2011 [14], as presented in Table 1.

Table 1. Physical properties of 70# base asphalt.

Properties	Result	Technical standard	Test method
Density ($\text{g}\cdot\text{cm}^{-3}$)	1.036	-	T0603
Penetration (25°C, 0.1 mm)	71	60~80	T0604
Softening point (°C)	47	> 46	T0606
Ductility (10°C, cm)	76	> 20	T0605

Three industrial granular anti-rutting additives, ARA-A, ARA-B and ARA-C (ARA is an abbreviation for anti-rutting additive, and A, B and C are marks that stand for different additives), were used to prepare modified asphalt binders. Figure 2 demonstrates the appearance of three additives, which are manufactured with a new mono-component epoxy and reactive tackifying resin. The specific composition of the three additives may be somewhat different. However, from the perspective of application in asphalt pavement, they all belong to the same category, namely, polymer modifiers.

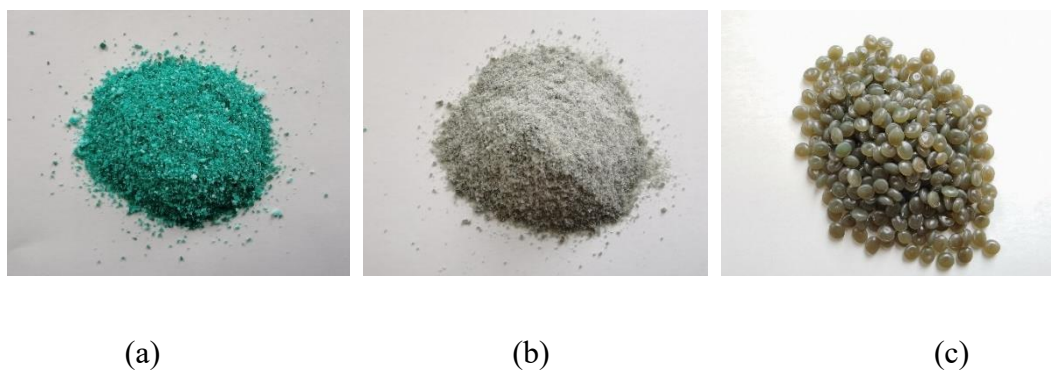


Figure 2. Appearance of three granular anti-rutting additives: (a) ARA-A, (b) ARA-B, (c) ARA-C.

Limestone was adopted for both coarse aggregate, fine aggregate and mineral powder. Their basic properties were tested according to JTG E42-2005 [15], as shown in Tables 2–4.

Table 2. Basic properties of coarse aggregates.

Technical indices	Test results	requirements	Test methods
Crushing value (%)	21	≤ 26	T 0316
Los Angeles Abrasion (%)	16.8	≤ 28	T 0317
Water absorption (%)	1.5	≤ 2.0	T 0304
Robustness (%)	3.5	≤ 12	T 0314
Soft stone content (%)	1.2	≤ 3.0	T 0320
Elongated particles content (%)	10.5	≤ 15	T 0312

Table 3. Basic properties of fine aggregates.

Technical indices	Test results	Requirements	Test methods
Mud content (%)	2.1	≤ 3	T 0333
Apparent relative density	2.635	≥ 2.50	T 0304
Sand equivalent (%)	76.7	≥ 60	T 0334
Robustness (%)	4.2	≤ 12	T 0340

Table 4. Basic properties of limestone powder.

Technical indices	Test result	Requirements	Test methods
Density ($\text{g}\cdot\text{cm}^{-3}$)	2.68	> 2.5	T0352
Hydrophilic coefficient	0.60	< 1	T0353
Moisture content (%)	0.18	< 1	T0103
BET specific surface area (m^2/g)	0.49	-	-

2.2. Preparation of modified binders and mixtures

In order to allow the additives to fully interact with the asphalt binder, a higher temperature (180°C) was conditioned to prepare ARA modified asphalts. A high-speed shearing machine was employed to efficiently shear the additives into tiny fragments so as to uniformly blend the mix. The rotation speed was 2000 r/min for preliminary blending, followed by 5000 r/min for shearing. Afterward, it was blended by a fan mixer at the rate of 1000 r/min to achieve a uniform phase state.

The Sup-13 was selected to design the gradation of asphalt mixtures, as shown in Figure 3. For anti-rutting asphalt mixtures, higher temperatures are required for both mixing and compaction, so that the additives have sufficient interaction between the asphalt and develop a considerable interlock and reinforcement with aggregate. The content of the ARA is 1% (mass ratio of additives to mixtures) according to the manufacturer's recommendation. Three types of ARAs were incorporated into the asphalt mixture by dry process, which implies additives were directly mixed with aggregates. During the preparing process, additives and aggregates were first mixed for 90 s to sufficiently soften the

ARAs. Following that, asphalt was added to mix for 90 s so that additives could fully react with the asphalt. Finally, mineral powder was introduced into the compound as the filler. As suggested in engineering examples, the mixing temperature was confined within 185 to 190°C and the compaction temperature was controlled within 175 to 180°C [12].

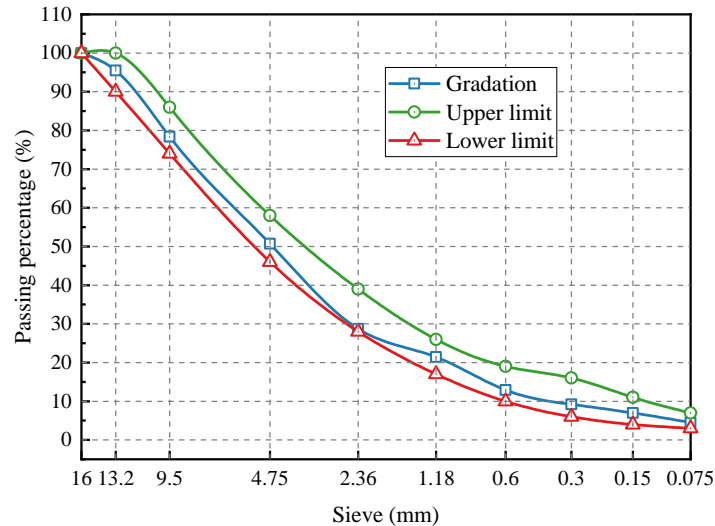


Figure 3. Gradation curve of Sup-13 mixture.

2.3. Test method

2.3.1. FM test

FM is a desirable approach to reveal the compatibility of asphalt and ARAs. The major form existing in the compounds includes the asphalt phase and additive phase. The distribution characteristics of additives in asphalt may cause a considerable difference in the compatibility of modified asphalts, thus generating a variation of road performances. To prepare the FM samples, the modified asphalt was first heated to a flow state (180°C), then a small amount of asphalt was dropped on a glass slide, followed by covering a cover glass. Afterward, when asphalt samples were cooled down, they were observed via the fluorescence microscope. The magnification is 100 times. The most representative FM images were captured.

2.3.2. MSCR test

To investigate the anti-rutting performance of the asphalt containing ARAs, the MSCR test was conducted under stress-recovery controlled mode at a high temperature (60°C) according to AASHTO TP 70. Total 20 cycles of 0.1 kPa shear stress were initially exerted on modified asphalt specimens, followed by 10 cycles of 3.2 kPa shear stress. Each cycle contained loading time for one second and strain recovery for nine second, respectively [16]. The recovery rate R of each cycle was utilized to characterize the ability of elastic recovery, as expressed in Eq (1). The non-recoverable creep compliance J_{nr} of each cycle was employed to study the resistance to permanent deformation, as given by Eq (2). Both R and J_{nr} are significant indicators to describe the anti-rutting performance of asphalt

at high temperature.

$$R = \frac{\varepsilon_c - \varepsilon_r}{\varepsilon_r - \varepsilon_0} \quad (1)$$

$$J_{nr} = \frac{\varepsilon_r - \varepsilon_0}{\sigma}, \quad (2)$$

where σ is the stress; ε_0 is the initial strain of each circle; ε_r is the strain after recovery of each circle; ε_c is the creep strain of each circle.

2.3.3. Wheel tracking test

Pavement rutting is generally induced by severe high temperatures and repeated wheel loads. The wheel tracking test is thereby extensively employed to simulate the formation of pavement rutting according to JTG E20-2011. To prepare the specimens of the wheel tracking test, each mixture was poured into a rectangular slab with the dimensions of 300 mm × 300 mm × 50 mm, as shown in Figure 4. Following that, the specimen was subjected to repeated wheel pressure of 0.7 MPa with a loading speed of 42 cycles/min for 60 min. The test was carried out at 60°C and the whole load period was 60 min. Eventually, dynamic stability (DS) was obtained to evaluate the anti-rutting performance of asphalt mixtures, which is calculated by using the rutting depth (RD) at 45 and 60 min, as shown in Eq (3).

$$DS = \frac{15 \times 42}{d_2 - d_1}, \quad (3)$$

where d_2 and d_1 are the RDs at the loading time of 60 and 45 min, respectively.



Figure 4. Specimen of track plate after testing.

3. Results and discussion

3.1. Analysis of modification mechanism between additives and asphalt

The dispersed state of additives in asphalt will strongly influence their compatibility. In general,

uniform fluorescent particles stand for desirable compatibility and accordingly indicate better modification effects on asphalt binder. Figure 5 presents four FM images of ARA modified asphalt. It is obvious that fluorescent particles appear in Figure 5(b)–(d), which are dispersed ARAs. Comparing various ARAs, the fluorescent particles in the image of ARA-A modified asphalt are relatively regular and uniform with large quantities. It indicates that ARA-A additives have formed a uniformly dispersed system with asphalt, behaving the beneficial compatibility. However, ARA-B modified asphalt indicates a slight difference with that of ARA-A, namely, less quantities of particles and larger sizes, so the ARA-B additive has relatively poor compatibility with asphalt. Notably, irregular fluorescent particles appear in ARA-C modified asphalt, showing elongated strip-type fluorescent particles, which may be attributed to the large size of the ARA-C additive, as described in Figure 5(d). However, it presents a large area of fluorescent particles in the ARA-C image, which implies the compatibility between the ARA-C and asphalt is acceptable. As a result, the compatibility between the asphalt and various additives fulfills the sequence: ARA-A > ARA-C > ARA-B.

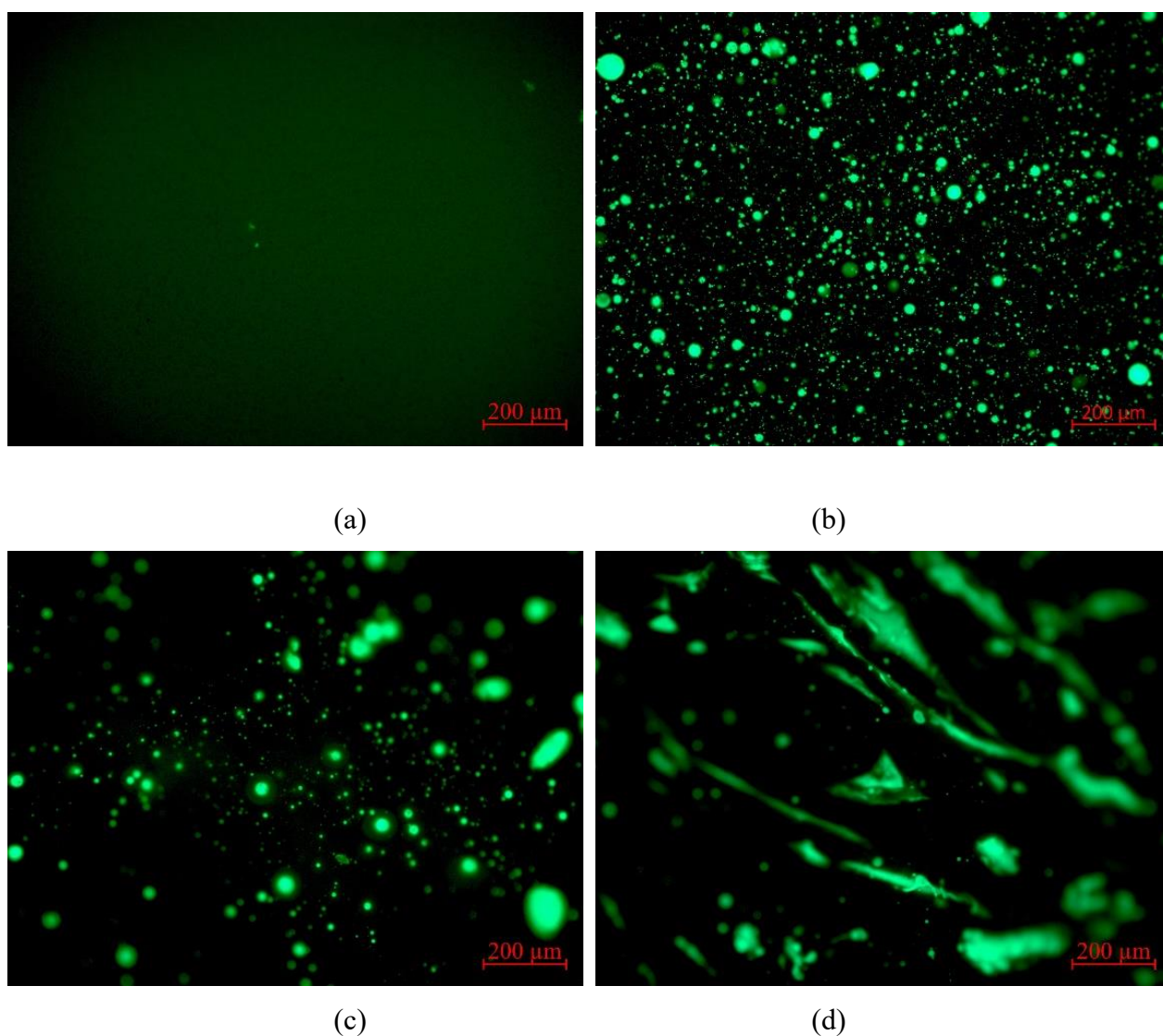


Figure 5. FM images of anti-rutting additive modified asphalt (magnification: 100): (a) 70#, (b) 70[#]-ARA-A, (c) 70[#]-ARA-B, (d) 70[#]-ARA-C.

3.2. Analysis of anti-rutting performance of asphalt binder based on MSCR test

The MSCR test was confirmed as a satisfactory approach for investigating the anti-rutting performance from the binder scale, in which the indicators R and J_{nr} highly correlate to the road performance [17]. A higher R and lower J_{nr} indicate better anti-rutting performance at a high temperature. Figure 6 presents shear strain-time curves of modified asphalts. The curves were obtained by applying 3.2 kPa. It is indicated that the incorporation of ARA-B additive leads to the minimum shear strain, followed by ARA-C and ARA-A, respectively. It implies that the deformation resistance under high temperature follows the sequence: ARA-B > ARA-C > ARA-A. Interestingly, the recoverable strain for ARA-B modified asphalt is obviously less than other two modified asphalts. This means the ARA-B modified asphalt has more sufficient elasticity characteristics.

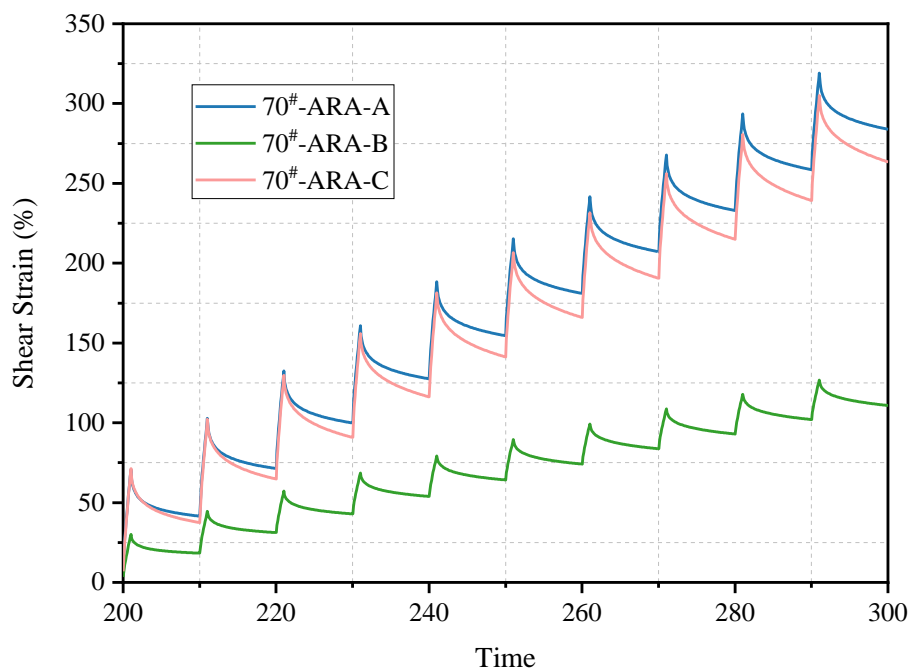


Figure 6. The relationship between shear strain and loading time.

The recovery rate R and non-recoverable creep compliance J_{nr} of different asphalts are presented in Figure 7. A remarkable increase of recovery rate is observed for the asphalt incorporating ARAs, with a maximum R up to 84.5% under 0.1 kPa and a maximum R up to 60.6% under 3.2 kPa. Notably, the recovery rates vary slightly for three types of modified asphalts. Similarly, a significant decrease in non-recoverable creep compliance is presented in Figure 7(b). It indicates that the resistance to unrecoverable deformation is dramatically improved for three modified asphalts.

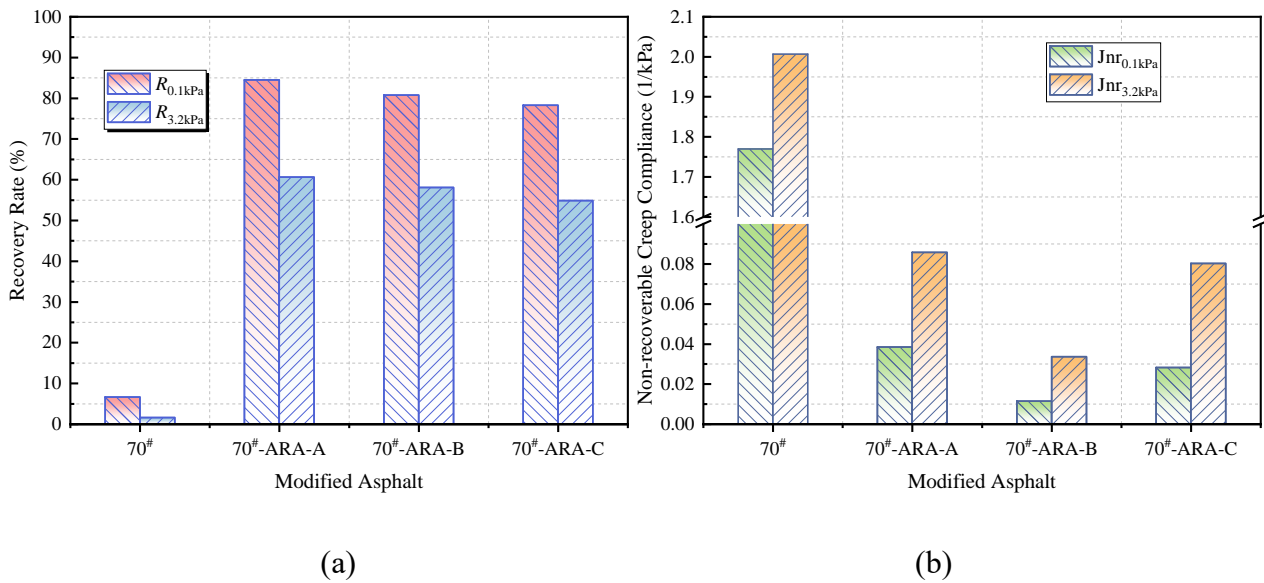


Figure 7. MSCR test results: (a) Recovery rate, (b) Non-recoverable creep compliance.

Based on the fluorescence microscopy experimental results, it is clear that the compatibility between the additive and the asphalt is not a decisive basis for determining the anti-rutting performance of modified asphalts. In fact, large quantities of ARAs are difficult to directly blend with asphalt, so the distribution characteristics of additives would not have a strong correlation with high-temperature anti-rutting performance. Under the circumstances, an in-depth investigation into the effects of additives on mixtures remains to be developed.

3.3. Analysis of DS error due to sensor accuracy

Wheel tracking test is widely applied to determine the anti-rutting performance of mixtures. After incorporating anti-rutting additives, asphalt mixtures generally have remarkable resistance to deformation, thereby the rutting depth obtained in wheel tracking test tends to be extremely small, nearly no more than 1mm. In particular, the deformation d_1 and d_2 would vary slightly during the loading period, which is hard to be detected by the machine sensor with low accuracy. The dynamic stability DS will then be affected, obtaining a deviated DS. As a result, the experimental errors caused by sensor accuracy demand in-depth investigation.

To calculate the DS error, a DS_1 is previously assumed, so the difference between d_1 and d_2 was obtained. Following that, given that the error might simultaneously happen to d_1 and d_2 or solely happen to one, the incorrect DS_2 was determined. Based on DS_1 and DS_2 , the relative errors of these two conditions were obtained, as shown in Figure 8(a)(b). It is found that the relative error gradually rises up with the increase of tested DS. Notably, the relative error due to both d_1 and d_2 increases more quickly than that due to one of them. Considering the uncertainty of errors, the possibility of both d_1 and d_2 having errors is bound to be high. For sensor accuracy ± 0.01 mm, when the DS of asphalt mixtures becomes 5250 cycle/mm, the relative error exceeds 20%, which is judged to have been an unacceptable error. For sensor accuracy ± 0.001 mm, when the DS is 53,000 cycle/mm, its relative error is regarded as an unacceptable error, exceeding 20%. It can be recognized that improving sensor accuracy would contribute to the reduction of test errors.

The findings imply that high-accuracy testing sensors are preferable to be employed for wheel

tracking testing. Furthermore, the variability of DS should be focused to ensure the result errors are within an acceptable range.

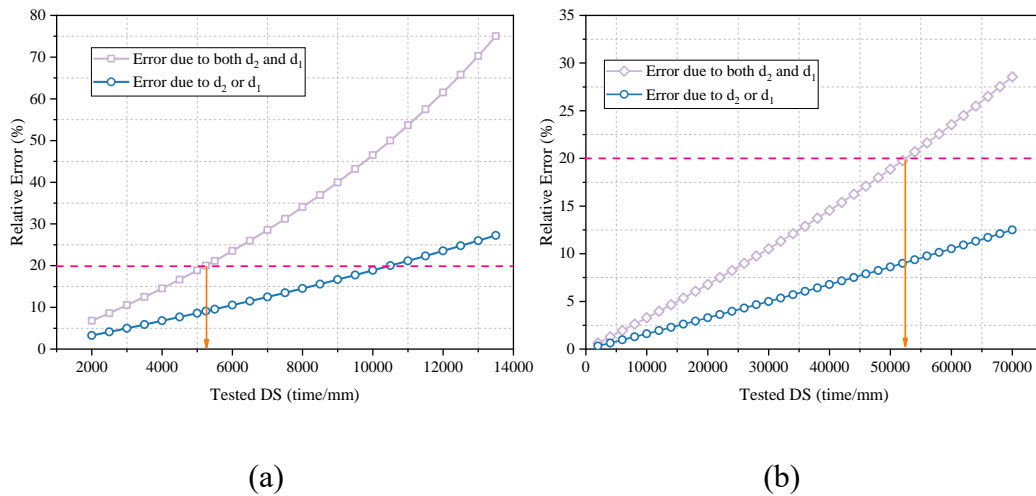


Figure 8. The relative error of DS due to sensor accuracy: (a) Sensor accuracy: ± 0.01 mm, (b) Sensor accuracy: ± 0.001 mm.

3.4. Anti-rutting performance of modified mixtures based on wheel tracking test

3.4.1. Rutting depth analysis

The rutting depth curve acquired from the wheel tracking test records the development process of rutting. As shown in Figure 9, the rutting deformation of various asphalt mixtures increases with time, including those modified with ARA-A, ARA-B and ARA-C. A deformation-strengthened type curve is observed for the relationship between rutting depth and time. The rutting depth first sharply increases during 0–10 min, then it increases at a slow rate during 10–60 min. The accumulation rutting depth of anti-rutting asphalt mixtures is rather small, for all modified SUP-13. The ARA-B modified SUP-13 has the minimum accumulation rutting depth, not exceeding 0.45 mm, which is mainly due to the modification of binders by additives and their reinforcement formed with aggregates.

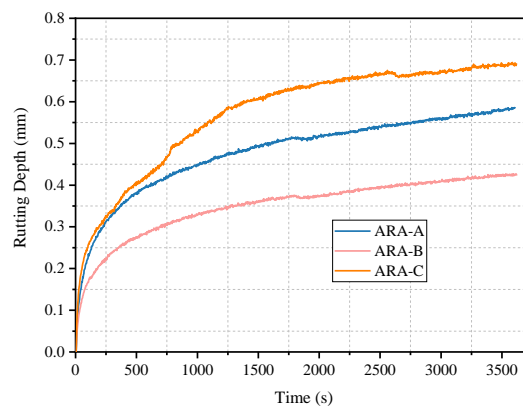


Figure 9. Rutting depth variation curve.

3.4.2. DS analysis

DS is a significant indicator to evaluate the anti-rutting performance of asphalt mixtures and reflect their resistance at the stable stage during rutting increase. A higher DS indicates the better high temperature performance. From Figure 10, it can be found that the DS of asphalt mixtures fulfills the sequence: SUP13-ARA-B > SUP13-ARA-A > SUP13-ARA-C > SUP13. Compared with SUP13, three modified asphalt mixtures have extremely larger DS, showing strong resistance to the rutting distress. Notably, the DS demonstrates larger variability for three modified asphalt mixtures, which is due to the error caused by sensor accuracy. Nonetheless, the maximum coefficient of variation of different modified asphalt mixtures is 16.5%, which is within 20%, so it is confirmed that the indicator DS is capable of reflecting the high-temperature performance of anti-rutting asphalt mixtures.

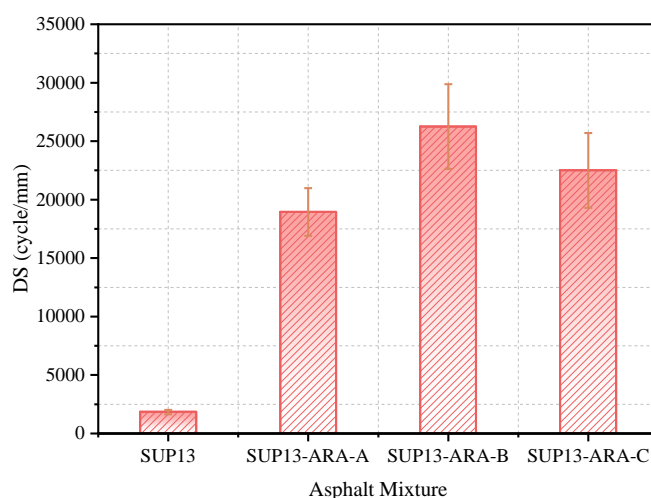


Figure 10. Dynamic stability obtained from the wheel tracking test.

3.5. Analysis of interaction between ARAs and asphalt mixtures

As described before, the ARA-A additive has the most desirable compatibility with the asphalt, followed by ARA-C and ARA-B, respectively. In most cases, the better compatibility implies more complete modification effects on the asphalt, thus leading to higher dynamic stability of the asphalt mixture. Nevertheless, three additives present differences in road performance. The main reasons could be traced back to the dry mixing process for preparing asphalt mixtures. The incorporation of ARAs into mixtures will not only interact with asphalt but also change their physical morphology [12], so ARAs mainly develop their functions via physical modification, instead of chemical reaction with aggregates.

Three ARAs in asphalt mixtures differ in their dynamic stability, which is mostly due to the various forms in which they are presented. The ARAs primarily achieve their function via two approaches. First, the melted ARA modifies the asphalt in a dispersed system. Second, the ARA, in a viscous-flow state, also has the effects of interlocking, filling voids, cementing and wrapping the aggregate, as presented in Figure 11. Accordingly, several stiff network structures are formed to confine the relative movement of mineral aggregates, as well as enhance the overall performance of the asphalt mixture.

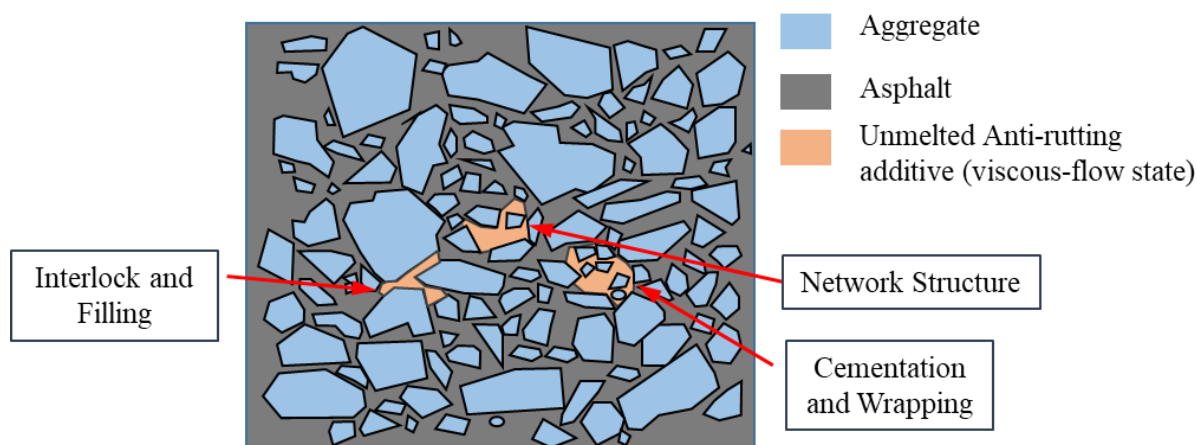


Figure 11. The interaction between the ARA and asphalt mixture.

The variation of road performance of different asphalt mixtures is due to the distribution form of ARAs. Large quantities of ARA-A additives are melted into the asphalt-additive system, so its leading intention is to improve the properties of asphalt. In contrast, a few quantities of ARA-C are melted into the asphalt, where it plays a more significant function in filling mineral voids and enhancing the overall performance of the asphalt mixture. More importantly, the latter has a greater impact on the dynamic stability of asphalt mixtures at a high temperature.

4. Conclusions

This study aimed to evaluate the effects of ARAs on the high-temperature performance of asphalt and asphalt mixtures. The FM test, MSCR test and wheel tracking test were conducted to reveal the performance of ARAs and their interactions with asphalt mixtures. The following main conclusions were drawn.

1) By incorporating ARA, a remarkable increase of recovery rate and a significant decrease of non-recoverable creep compliance were observed for the asphalt.

2) Fluorescent particles were uniformly presented with large quantities in the FM image of ARA-A modified asphalt, which implies good compatibility. The compatibility between the asphalt and various additives fulfill the sequence: ARA-A > ARA-C > ARA-B.

3) Due to differences in dispersion characteristics, the compatibility between the additive and the asphalt binder was not the only leading factor that correlated with their high-temperature anti-rutting performance.

4) ARAs hugely raise the dynamic stability of mixtures. Melted ARAs modify the asphalt to improve the performance of asphalt mixtures. Further, viscous-flow additives contribute to the modification of asphalt mixtures by interlock action, filling voids, cementing and wrapping the aggregate.

In the future, extensive research efforts will be made to investigate the comprehensive performances of asphalt mixtures due to the incorporation of ARAs. Further, developing a quantitative relationship between the performance and the distribution form of ARAs will be performed in the follow-up studies.

Use of AI tools declaration

The authors declare they have not used Artificial Intelligence (AI) tools in the creation of this article.

Acknowledgments

This research was funded by the Opening Project of National Engineering Research Center of Advanced Road Materials (Grant No. 22990169).

Conflict of interest

The authors declare there is no conflict of interest.

References

1. Y. Jia, S. Wang, J. Peng, Y. Gao, D. Hu, X. Zhao, Evaluation of pavement rutting based on driving safety of vehicles, *Int. J. Pavement Res. Technol.*, **15** (2022), 457–469. <https://doi.org/10.1007/s42947-021-00032-2>
2. J. S. Tong, T. Ma, K. R. Shen, H. Y. Zhang, S. P. Wu, A criterion of asphalt pavement rutting based on the thermal-visco-elastic-plastic model, *Int. J. Pavement Eng.*, **23** (2020), 4. <https://doi.org/10.1080/10298436.2020.1792470>
3. Y. Luan, Y. Ma, T. Ma, C. Wang, F. Xia, Research on the effects of asphalt performance on rutting resistance and its correlation with rutting performance indicators, *Constr. Build. Mater.*, **400** (2023), 132773. <https://doi.org/10.1016/j.conbuildmat.2023.132773>
4. R. S. McDaniel, H. U. Bahia, Field evaluation of asphalt additives to control rutting and cracking, *Transp. Res. Record*, **1829** (2003), 47–54. <https://doi.org/10.3141/1829-07>
5. A. K. Ghuzlan, W. B. Al-Mistarehi, S. A. Al-Momani, Rutting performance of asphalt mixtures with gradations designed using Bailey and conventional Superpave methods, *Constr. Build. Mater.*, **261** (2020), 119941. <https://doi.org/10.1016/j.conbuildmat.2020.119941>
6. J. Yang, J. Cui, J. Wan, X. Shi, Strategy of improving rutting resistance based on contribution rate of different layers, *J. Southeast Univ. (Nat. Sci. Ed.)*, **37** (2007), 350–354. <https://doi.org/10.3969/j.issn.1001-0505.2007.02.033>
7. Y. L. Zhang, N. Li, Research on applicability of anti-rutting agent LY to different asphalt mixtures, in *IOP Conference Series: Earth and Environmental Science*, **587** (2020), 1. <https://doi.org/10.1088/1755-1315/587/1/012029>
8. W. J. Wang, *Design of Key Parameters and Study on the Performance of Bituminous Mixtures Mixed with Anti-Rutting Additive*, M.S. thesis, Chang'an University, 2011.
9. Z. Q. Zhang, Y. F. Luo, K. Zhang, Research on influence of different anti-rutting additives on high-temperature performance of asphalt mixture, *J. Railw. Sci. Eng.*, **14** (2017), 964–970. <https://doi.org/10.19713/j.cnki.43-1423/u.2017.05.012>
10. Y. S. Guan, H. Li, Z. X. Zhang, X. Y. Li, A new high rutting resistance asphalt mixture for intersection maintenance under heavy traffic, *J. Test. Eval.*, **40** (2012), 1156–1161. <https://doi.org/10.1520/JTE20120126>

11. B. Wang, X. D. Hu, C. F. Cao, J. M. Wan, W. X. Gan, Z. W. Chen, et al., Development and characterization of permeative anti-rutting agent for asphalt mixture enhancement, *Constr. Build. Mater.*, **364** (2023), 129937. <https://doi.org/10.1016/j.conbuildmat.2022.129937>
12. S. Han, W. Y. Ren, J. X. Jia, H. Yang, D. Y. Niu, Study on road performances of asphalt mixtures with granulated polymer anti-rutting additive, *Int. J. Pavement Eng.*, **21** (2020), 257–265. <https://doi.org/10.1080/10298436.2018.1461868>
13. F. P. Xiao, D. F. Ma, J. Y. Wang, D. G. Cai, L. W. Lou, J. Yuan, Impacts of high modulus agent and anti-rutting agent on performances of airfield asphalt pavement, *Constr. Build. Mater.*, **204** (2019), 1–9. <https://doi.org/10.1016/j.conbuildmat.2019.01.138>
14. JTG E20-2011, *Standard Test Methods of Bitumen and Bituminous Mixtures for Highway Engineering*, Ministry of Transport of the People’s Republic of China, 2011.
15. JTG E42-2005, *Test Methods of Aggregate for Highway Engineering*, Ministry of Transport of the People’s Republic of China, 2005.
16. Z. Y. Wei, Y. S. Jia, S. Q. Wang, Z. R. Li, Y. S. Li, X. M. Wang, et al., Utilization of iron ore tailing as an alternative mineral filler in asphalt mastic: High-temperature performance and environmental aspects, *J. Cleaner Prod.*, **335** (2022), 130318. <https://doi.org/10.1016/j.jclepro.2021.130318>
17. M. D. I. Domingos, A. L. Faxina, Susceptibility of asphalt binders to rutting: Literature review, *J. Mater. Civ. Eng.*, **28** (2016), 04015134. [https://doi.org/10.1061/\(ASCE\)MT.1943-5533.0001364](https://doi.org/10.1061/(ASCE)MT.1943-5533.0001364)



AIMS Press

©2024 the Author(s), licensee AIMS Press. This is an open access article distributed under the terms of the Creative Commons Attribution License (<http://creativecommons.org/licenses/by/4.0>)